New Precursors for Barium Metal-Organic Chemical Vapor Deposition. In Situ Growth of Epitaxial Barium Titanate Films Using a Liquid Barium Precursor

Deborah A. Neumayer,[†] Daniel B. Studebaker, Bruce J. Hinds, Charlotte L. Stern, and Tobin J. Marks*
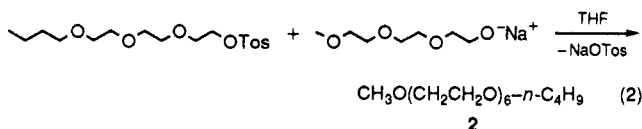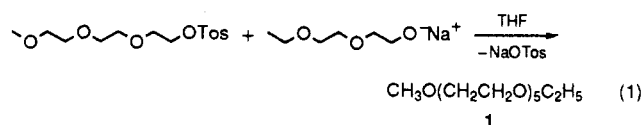
*Department of Chemisty
The Materials Research Center and the
Science and Technology Center for Superconductivity
Northwestern University
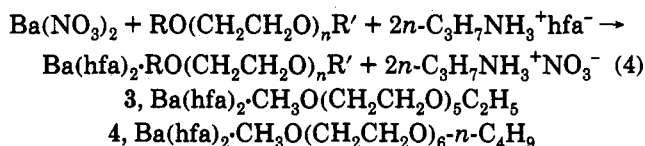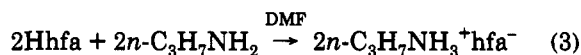Evanston, Illinois 60208-3113*

Film growth by MOCVD (metal–organic chemical vapor deposition) of barium-containing HTS[1-3] (high-temperature superconducting) and defect-free ferroelectric/photonic[4] materials is crucially dependent upon the availability of molecular barium–organic precursors having high and stable vapor pressures as well as appropriate reactivity under film growth conditions. Substantial progress has recently been made using coordination sphere-saturating (to maintain monomeric structures) β-diketonate ligation ensembles,[5] with "second-generation" complexes as exemplified by Ba(hfa)$_2$·tetraglyme (hfa = hexafluoroacetylacetonate)[1,6] receiving considerable attention. However, such precursors typically have high melting points and must be utilized for film growth in the temperature range where they are solids (decomposition and unstable vapor pressure occur at higher temperatures). In principal, liquid MOCVD precursors would offer greater film growth

efficiency and vapor pressure stability since there is more effective vapor pressure equilibration with the carrier gas stream and no unpredictable, time-varying dependence of sublimation characteristics on solid surface area and sintering effects.[7] We report here on the synthesis, structural properties, and transport characteristics of the first volatile, low melting point Ba(hfa)$_2$·polyether MOCVD precursors[8] as well as their implementation for the *in situ* growth of epitaxial films of the nonlinear optical material BaTiO$_3$.

The symmetry-breaking polyethers 2,5,8,11,14,17-hexaoxanonadecane (1) and 2,5,8,11,14,17,20-heptaoxatetracosane (2) were prepared from the appropriate oligoethylenegylcol monoalkyl ether alkoxides and tosylates following a modified literature procedure (eqs 1 and 2).[9] The Ba(hfa)$_2$·polyether complexes were then syn-

$$\text{(1)} \qquad CH_3O(CH_2CH_2O)_5C_2H_5$$

$$\text{(2)} \qquad CH_3O(CH_2CH_2O)_6\text{-}n\text{-}C_4H_9$$

thesized from 99.999% Ba(NO$_3$)$_2$ dissolved in polyether, DMF, and water by addition of an hfa$^-$ solution in n-propylamine + DMF[10] (eqs and 4). Complex 3 was

$$2Hhfa + 2n\text{-}C_3H_7NH_2 \xrightarrow{\text{DMF}} 2n\text{-}C_3H_7NH_3{}^+hfa^- \quad (3)$$

$$Ba(NO_3)_2 + RO(CH_2CH_2O)_nR' + 2n\text{-}C_3H_7NH_3{}^+hfa^- \rightarrow$$

$$Ba(hfa)_2\text{·}RO(CH_2CH_2O)_nR' + 2n\text{-}C_3H_7NH_3{}^+NO_3{}^- \quad (4)$$

3, Ba(hfa)$_2$·CH$_3$O(CH$_2$CH$_2$O)$_5$C$_2$H$_5$
4, Ba(hfa)$_2$·CH$_3$O(CH$_2$CH$_2$O)$_6$-n-C$_4$H$_9$

[†] Present address: Science and Technology Center for Electronic Materials Growth, Department of Chemistry, University of Texas, Austin, TX 78712.

(1) (a) Malandrino, G.; Richeson, D. S.; Marks, T. J.; DeGroot, D. C.; Kannewurf, C. R. *Appl. Phys. Lett.* 1991, 58, 182. (b) Zhang, J. M.; Wessels, B. W.; Richeson, D. S.; Marks, T. J.; DeGroot, D. C.; Kannewurf, C. R. *J. Appl. Phys.* 1991, 69, 2743. (c) Duray, S. J.; Buchholz, D. B.; Song, S. N.; Richeson, D. S.; Ketterson, J. B.; Marks, T. J.; Chang, R. P. H. *Appl. Phys. Lett.* 1991, 59, 1503. (d) Zhang, J.; Zhao, J.; Marcy, H. O.; Tonge, L. M.; Wessels, B. W.; Marks, T. J.; Kannewurf, C. R. *Appl. Phys. Lett.* 1989, 54, 1166. (e) Richeson, D. S.; Tonge, L. M.; Zhao, J.; Zhang, J.; Marcy, H. O.; Marks, T. J.; Wessels, B. W.; Kannewurf, C. R. *Appl. Phys. Lett.* 1989, 54, 2154.

(2) (a) Zhang, K.; Erbil, A. *Mater. Sci. Forum* 1993, 130–132, 255 and references therein. (b) Hirai, T.; Yamane, H. *J. Cryst. Growth* 1991, 107, 683 and references therein.

(3) (a) Zhao, J.; Li, Y. Q.; Chern, C. S.; Lu, P.; Norris, P.; Gallois, B.; Kear, B.; Cosandey, F.; Wu, X. D.; Muenchausen, R. E.; Garrison, S. M. *Appl. Phys. Lett.* 1991, 59, 1254. (b) Spee, C. I. M. A.; Vander Zouwen-Assink, E. A.; Timmer, K.; Mackor, A.; Meinema, H. A. *J. Phys. IV* 1991, 1, C2/295.

(4) (a) Lu, H. A.; Wills, L. A.; Wessels, B. W.; Lin, W. P.; Zhang, T. G.; Wong, G. K.; Neumayer, D. A.; Marks, T. J. *J. Appl. Phys. Lett.* 1993, 62, 1314. (b) Wills, L. A.; Wessels, B. W.; Richeson, D. S.; Marks, T. J. *Appl. Phys. Lett.* 1992, 60, 41. (c) Van Buskirk, P. C.; Gardiner, R.; Kirlin, P. S.; Nutt, S. *J. Mater. Res.* 1992, 7, 542. (d) Chern, C. S.; Zhao, J.; Luo, L.; Lu, P.; Li, Y. Q.; Norris, P.; Kear, B.; Cosandey, F.; Maggiore, C. J.; Ballois, B.; Wilkens, B. *J. Appl. Phys. Lett.* 1992, 9, 1144. (e) Kwak, B. S.; Zhang, K.; Boyd, E. P.; Erbil, A; Wilkens, B. J. *J. Appl. Phys.* 1991, 2, 767.

(5) (a) Schulz, D. L.; Hinds, B. J.; Neumayer, D. A.; Stern, C. L.; Marks, T. J. *Chem. Mater.* 1993, 5, 1605 and references therein. (b) Rees, Jr., W. S.; Caballero, C. R.; Hesse, W. *Angew. Chem., Int. Engl. Ed.* 1992, 31, 735. (c) Gardiner, R.; Brown, D. W.; Kirlin, P. S.; Rheingold, A. L. *Chem. Mater.* 1991 3, 1053. (d) Tonge, L. M.; Richeson, D. S.; Marks, T. J.; Zhao, J.; Zhang, J.; Wessels, B.W.; Marcy, H. O.; Kannewurf, C. R. *Adv. Chem. Ser.* 1990, 226, 351.

(6) (a) Timmer, K.; Spee, C. I. M. A.; Mackor, A.; Meinema, H. A.; Spek, A. L.; van der Sluis, P. *Inorg. Chim. Acta* 1991, 190, 109. (b) Van der Sluis, P.; Spee, A. L.; Timmer, K.; Meinema, H. A. *Acta Crystallogr.* 1990, C46, 1741.

(7) Kuech, T. F.; Jensen, K. F. In *Thin Film Processes II;* Vossen, J. L., Kern, W., Eds.; Academic Press: Boston, MA, 1991, Vol. 3, p 377.

(8) For a recently reported, alternative approach to a low-melting Ba precursor, see: Sarkis, S. H.; Hitchman, M. L.; Cook, S. L.; Richards, B. G. *J. Mater. Chem.* 1994, 4, 81.

(9) Dale, J.; Kristiansen, P. O. *Acta Chem. Scand.* 1972, 26, 1471.

(10) This nonaqueous medium avoids hydration of Hhfa: Schulz, D. L.; Neumayer, D.A.; Marks, T. J. *Inorg. Synth.*, in press.

(11) Spectroscopic and analytical data for 3: ^{1}H NMR (300 MHz, CDCl$_3$) δ 0.85 (m, 3H, CH$_3$), 3.27 (s, 3H, OCH$_3$), 3.42 (m, 2H, OCH$_2$), 3.56 (m, 12H, OCH$_2$), 3.70 (m, 8H, OCH$_2$), 5.77 (s, 2H, CH) . ^{13}C NMR (75 MHz, CDCl$_3$) δ 174.2 (q, 31.3 Hz, CO), 118.3 (q, 288.0 Hz, CF$_3$), 86.2 (q, 7.3 Hz, CH), 72.2 (s, OCH$_2$), 70.5 (s, OCH$_2$), 70.2 (s, OCH$_2$), 70.0 (s, OCH$_2$), 69.9 (s, OCH$_2$), 69.7 (s, OCH$_2$), 69.6 (s, OCH$_2$), 69.2 (s, OCH$_2$), 68.5 (s, OCH$_2$), 66.1 (s, OCH$_2$), 58.9 (s, OCH$_2$), 13.6 (s, CH$_3$) . ^{19}F NMR (282 MHz, CDCl$_3$): δ -77.29 (s). Anal. Calcd for C$_{23}$H$_{30}$O$_{10}$F$_{12}$Ba: C, 33.21; H, 3.65. Found: C, 32.97; H, 3.56. MS (EI$^+$, 70 eV, m/z^+; fragment L = C$_{13}$H$_{28}$O$_6$): 831 (P), 669 (P − C$_7$H$_{15}$O$_4$), 653 (P − hfa), 465 (BaF·L), 345 (Ba(hfa)), 223 (P − 2hfa), 208 (hfa), 157 (BaF).

(12) Spectroscopic and analytical data for 4: ^{1}H NMR (300 MHz, CDCl$_3$) δ 0.82 (m, 3H, CH$_3$), 1.20 (m, 2H, CH$_2$), 1.43 (m, 2H, CH$_2$), 3.20 (s, 3H, OCH$_3$), 3.31 (m, 2H, OCH$_2$), 3.42 (m, 2H, OCH$_2$), 3.46 (m, 2H, OCH$_2$), 3.53 (s, 12H, OCH$_2$), 3.60 (s, 8H, OCH$_2$), 5.73 (s, 2H, CH) . ^{13}C NMR (75 MHz, CDCl$_3$) δ 175.2 (q, 30.9 Hz, CO), 118.1 (q, 288.6 Hz, CF$_3$), 86.0 (CH), 71.2 (s, OCH$_2$), 70.8 (s, OCH$_2$), 69.9 (s, OCH$_2$), 69.4 (s, OCH$_2$), 69.35 (s, OCH$_2$), 69.26 (s, OCH$_2$), 69.2 (s, OCH$_2$), 69.0 (s, OCH$_2$), 68.9 (s, OCH$_2$), 68.5 (s, OCH$_2$), 68.3 (s, OCH$_2$), 68.1 (s, OCH$_2$), 58.6 (s, OCH$_3$), 30.8 (s, CH$_2$), 18.9 (s, CH$_2$), 13.7 (s, CH$_3$) . ^{19}F NMR (282 MHz, CDCl$_3$) δ -76.62 (s). Anal. Calcd for C$_{27}$H$_{38}$O$_{11}$F$_{12}$Ba: C, 35.88; H, 4.21. Found: C, 36.21; H, 4.46. MS (EI$^+$, 70 eV, m/z^+; L = C$_{17}$H$_{36}$O$_7$): 860 (P − C$_2$H$_5$O), 741 (P − C$_7$H$_{15}$O$_4$), 697 (P − hfa), 509 (BaF·L), 375 (BaF·L − C$_6$H$_{13}$O$_3$), 345 (Ba(hfa)), 245 (P − 2hfa), 208 (hfa), 157 (BaF).

　　　© 1994 American Chemical Society

Communications

Chem. Mater., Vol. 6, No. 7, 1994 879
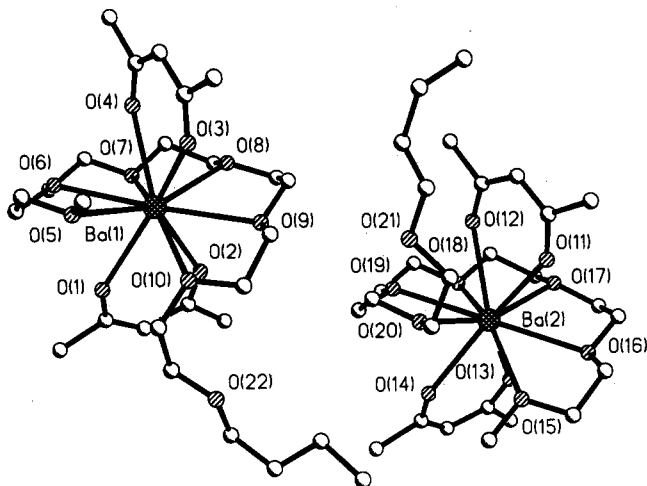
Figure 1. Perspective view of the solid state structure of Ba-$(hfa)_2 \cdot CH_3O(CH_2CH_2O)_6$-$n$-$C_4H_9$ (**4**) showing the two independent molecules in the unit cell. Important bond distances (angles) and angles (degrees) are $Ba(1)-O(1) = 2.765(5)$, $Ba(1)-O(2) = 2.803(5)$, $Ba(1)-O(3) = 2.734(5)$, $Ba(1)-O(4) = 2.773(5)$, $Ba(1)-O(5) = 2.833(5)$, $Ba(1)-O(6) = 2.850(5)$, $Ba(1)-O(7) = 2.828(5)$, $Ba(1)-O(8) = 2.817(5)$, $Ba(1)-O(9) = 2.872(5)$, $Ba(1)-O(10) = 2.823(5)$, $Ba(2)-O(11) = 2.792(6)$, $Ba(2)-O(12) = 2.776(6)$, $Ba(2)-O(13) = 2.807(6)$, $Ba(2)-O(14) = 2.712(5)$, $Ba(2)-O(15) = 2.828(5)$, $Ba(2)-O(16) = 2.860(5)$, $Ba(2)-O(17) = 2.810(5)$, $Ba(2)-O(18) = 2.850(5)$, $Ba(2)-O(19) = 2.853(5)$, $Ba(2)-O(20) = 2.883$ (6); $O(1)-Ba(1)-O(2) = 62.4(1)$, $O(3)-Ba(1)-O(4) = 62.2(2)$, $O(11)-Ba(2)-O(12) = 61.3(2)$, $O(13)-Ba(2)-O(14) = 63.0(2)$.

purified by repeated sublimation at 100 °C/0.05 Torr (70% yield), while **4** was recrystallized from hot heptane (50% yield). Both complexes were characterized by standard spectroscopic/analytical techniques[11,12] and **4** by single-crystal X-ray diffraction (*vide infra*). Complexes **3** and **4** melt at 109–110 and 52–54 °C, respectively, which can be compared to 151–152 °C for $Ba(hfa)_2 \cdot$tetraglyme.

The solid-state structure of complex **4**[13] consists of two monomeric, crystallographically independent, 10-coordinate (distorted bicapped square antiprismatic) Ba-$(hfa)_2 \cdot CH_3O(CH_2CH_2O)_6$-$n$-$C_4H_9$ molecules (Figure 1). The hexacoordinate (only 6 of 7 oxygen atoms are coordinated to Ba^{+2}) polyether ligand is disposed in a meridional girdle about the Ba^{+2} ion with the bidentate hfa⁻ ligands arrayed above and below this plane. A similar ligation motif is seen in 9-coordinate $Ba(hfa)_2 \cdot$tetraglyme[6b] and in 10-coordinate $Ba(hfa)_2 \cdot$18-crown-6.[14] Indeed, the present Ba–O(hfa) and Ba–O(ether) distances are unexceptional in comparison to these structures. The two $BaO_2(hfa)$ planes in **4** are staggered by 82.0(4)°, which compares favorably to the former two complexes.

In regard to vapor-phase barium transport characteristics, atmospheric pressure TGA[15a] measurements reveal that **3** and $Ba(hfa)_2 \cdot$tetraglyme behave similarly under these conditions: T(50% weight loss) = 272 and 261 °C;

Figure 2. Low pressure TGA data (6 Torr) comparing Ba-$(hfa)_2 \cdot$MEP (complex **3**) and $Ba(hfa)_2 \cdot$tetraglyme sublimation rates as a function of temperature..

(a)

(b)
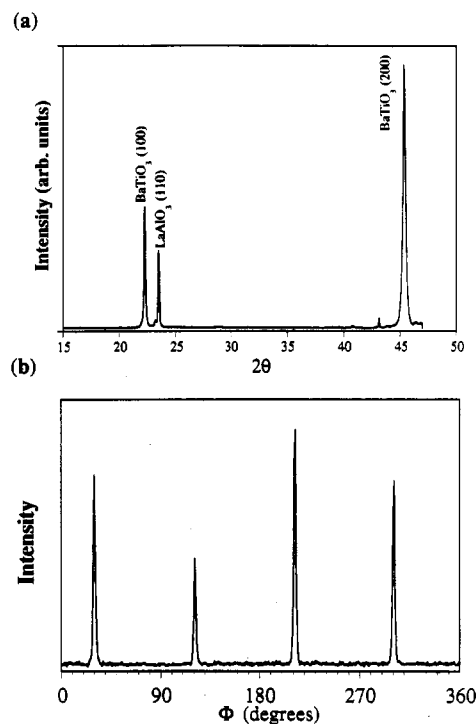
Figure 3. (a) X-ray diffraction θ–2θ scan of an epitaxial $BaTiO_3$ film grown *in situ* on a single-crystal (110) $LaAlO_3$ substrate by MOCVD using **3** and titanium tetraethoxide as precursors. (b) X-ray diffraction in-plane ϕ scan of an epitaxial $BaTiO_3$ film grown *in situ* on a single-crystal (110) $LaAlO_3$ substrate by MOCVD using **3** and titanium tetraethoxide.

% residue = 14 and 16, respectively. Complex **4** is somewhat less volatile as indicated by corresponding parameters of 260 °C and 19. Low-pressure sublimation rate TGA experiments (Figure 2)[15b] show that complex **3** sublimes ca. 3× more rapidly than $Ba(hfa)_2 \cdot$tet under typical MOCVD film growth conditions (120 °C/6 Torr).

MOCVD experiments were carried out in a horizontal quartz low-pressure reactor having thermostated Pyrex external precursor reservoirs and an internal, 2 × 6 × 20

(13) Crystal data for **4**: $C_{27}H_{38}F_{12}O_{11}Ba$, triclinic, $P\bar{1}$ No. 2), $a = 12.380$ (2) Å, $b = 19.076$ (2) Å, $c = 19.133$ (2) Å, $\alpha = 119.55$ (1)°, $\beta = 90.24$ (2)°, $\gamma = 107.24$°, $V = 3692$ (3) Å³, $Z = 4$, FW = 903.90; $\rho = 1.626$ g/cm³, μ(Mo Kα) = 11.8 cm⁻¹, $T = -120$ °C. Of 10 800 data collected ($2\theta_{max} = 46$°, Enraf-Nonius CAD-4), 10,237 were unique ($R_{int} = 0.038$). The final cycle of least-squares refinement was based on 7365 observed reflections ($I > 3.00\sigma(I)$) and 924 variable parameters and converged (largest parameter shift was 0.77 times its esd) with weighted and unweighted agreement factors of $R = 0.043$ and $R_w = 0.054$. All calculations were performed using the TEXSAN (TEXRAY Structure Analysis Package, 1985) crystallographic software package of Molecular Structure Corp. Further data are contained in the supplementary material.

(14) Norman, J. A. T.; Pez, G. P. *J. Chem. Soc., Chem. Comm.* **1991**, 971.
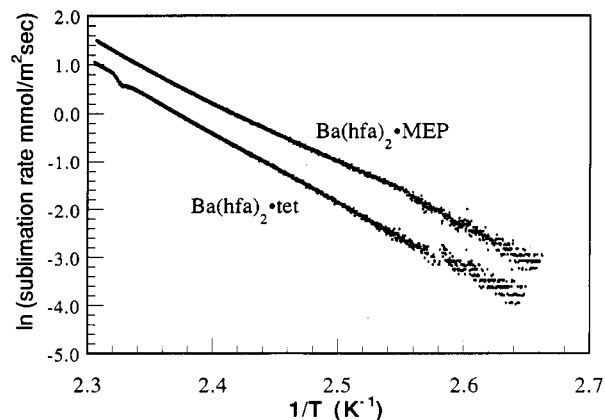
(15) (a) Flowing N_2 with a temperature ramp of 10 °C/min. (b) Experiments were performed with a temperature ramp of 1.5 °C/min, N_2 as the carrier gas, and with a 4-mm-diameter Pt sample pan. At this pressure, the sublimation rate is likely determined by both intrinsic vapor pressure characteristics and mass transfer into the carrier gas stream.

(16) Hinds, B. J.; Schulz, D. L.; Neumayer, D. A.; Han, B.; Marks, T. J.; Wang, Y. Y.; Dravid, V. P.; Schindler, J. L.; Hogan, T. P.; Kannewurf, C. R. *Appl. Phys. Lett.*, in press.

880 *Chem. Mater., Vol. 6, No. 7, 1994*

Communications

cm rectangular quartz laminar flow chamber leading to a radiantly heated graphite susceptor.[1a,16] For *in situ* epitaxial BaTiO$_3$ growth on clean (110) LaAlO$_3$ substrates, 3 maintained at 116 °C (liquid) and [Ti(OC$_2$H$_5$)$_4$]$_n$ at 68 °C (liquid) were transported in flowing Ar (100 sccm). An H$_2$O-saturated O$_2$ reactant gas stream was introduced immediately upstream of the film growth zone. The overall system pressure was 3 Torr, and the susceptor temperature was 775 °C. Typical film growth rates were ~1 μm/h. The resulting BaTiO$_3$ films are visually mirror smooth. X-ray diffraction θ–2θ scans (Figure 3a) indicate phase-pure films with a high degree of (100) growth orientation. The high degree of growth plane alignment is further confirmed by ω-scan rocking curves which indicate a full-width at half-maximum for the BaTiO$_3$ (200) reflection of 0.51° (vs 0.20° for the LaAlO$_3$ substrate (220) reflection). In-plane ϕ scans (Figure 3b) of the $\langle 220 \rangle$ family of BaTiO$_3$ diffraction planes exhibit sharp reflections every 90°, consistent with 4-fold symmetry and a high degree of in-plane epitaxy. Auger sputtering experiments[17] indicate that residual F$^-$ in the films (presumably derived from the hfa ligands) is below the instrumental detection limits ($\lesssim$0.5 atom %).

In regard to utility in high throughput MOCVD, we find that samples of 3 can be employed nearly continuously over periods of several months for film growth experiments without detectable degradation in vapor pressure/transport characteristics. Under the same conditions, solid Ba-(hfa)$_2$·tetraglyme samples undergo appreciable loss in volatility which can be restored (after growth interruption) only by retrieving and pulverizing the sintered samples.

In summary, these results demonstrate that volatile barium β-diketonate MOCVD precursors are synthetically accessible which allow efficient metal oxide film growth from the precursor liquid state. In the case of BaTiO$_3$ films, phase-pure epitaxial growth is achieved. It is anticipated that these new precursors will prove especially useful in experiments where reproducible, fine control of precursor vapor pressure is essential, such as in pulsed organometallic beam epitaxy (POMBE) of multilayer structures.[1c,18]

Supplementary Material Available: Complete list of crystallographic data, atom positions, and thermal parameters (14 pages); listing of observed and calculated structure factors (50 pages). Ordering information is given on any current masthead page.

(17) Physical Electronics Industries scanning Auger microprobe (3 keV). Sputtering was carried out to a depth of 100 Å.

(18) Duray, S. J.; Buchholz, D. B.; Zhang, H.; Song, S. N.; Schulz, D. L.; Dravid, V. P.; Marks, T. J.; Ketterson, J. B.; Chang, R. P. H. *J. Vac. Sci. Technol. A* **1993**, *11*, 1346 and references therein.